GREAT DESIGNS IN STEEL

Sumitomo Heavy Industries, Ltd. × UNIVERSITY OF MICHIGAN

JOINT RESEARCH PROGRAM

Multi-Forming Structures (MFS): A STAF®-Based Approach to Higher Stiffness and Lower CO_2

Sumitomo Heavy Industries Ltd.
Ryuichi Funada, Global Business Development Team Lead
University of Michigan
Kazuhiro Saitou, Professor of Mechanical Engineering

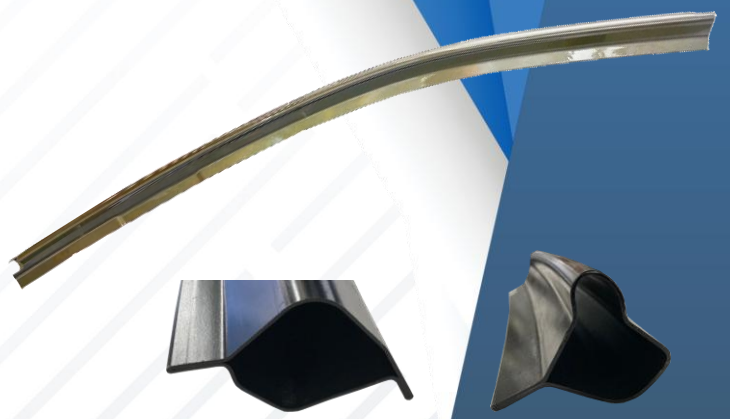

Table of Contents

What is STAF® *Steel Tube Air Forming* ?

GDIS

How STAF® Works *Steel Tube Air Forming* ?

GDIS

- **Simultaneous flange forming** - eliminating secondary operations
- **Robust, cost-efficient resistance heating** fully integrated into the press system
- Closed-section design | Increased stiffness | >TS1500MPa | Tailored sections

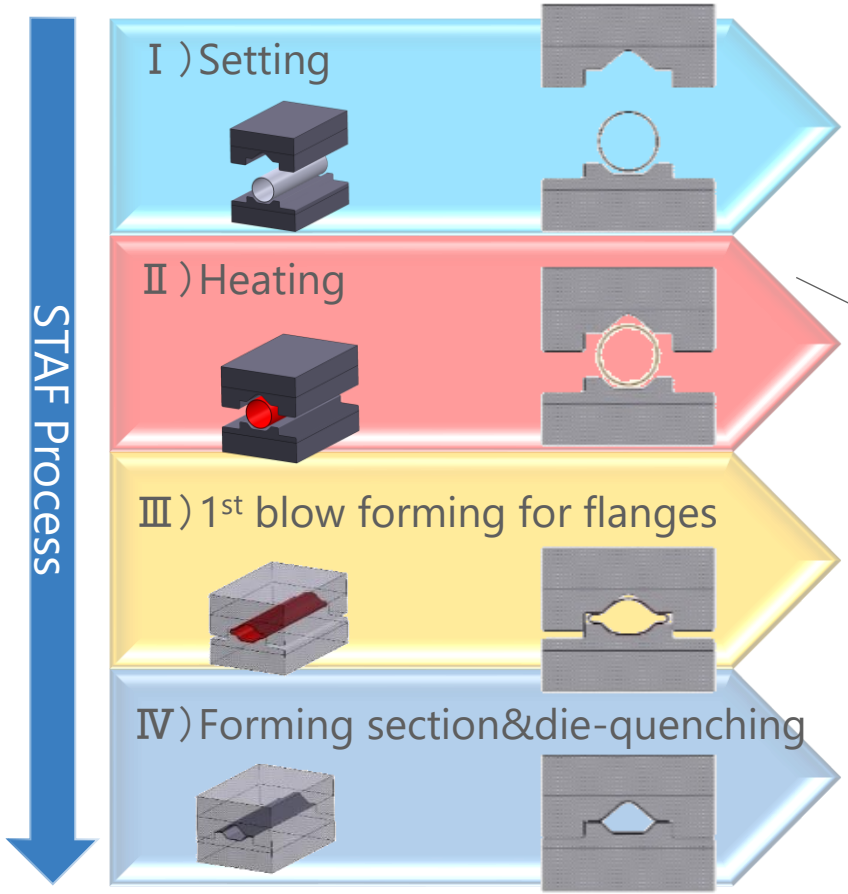

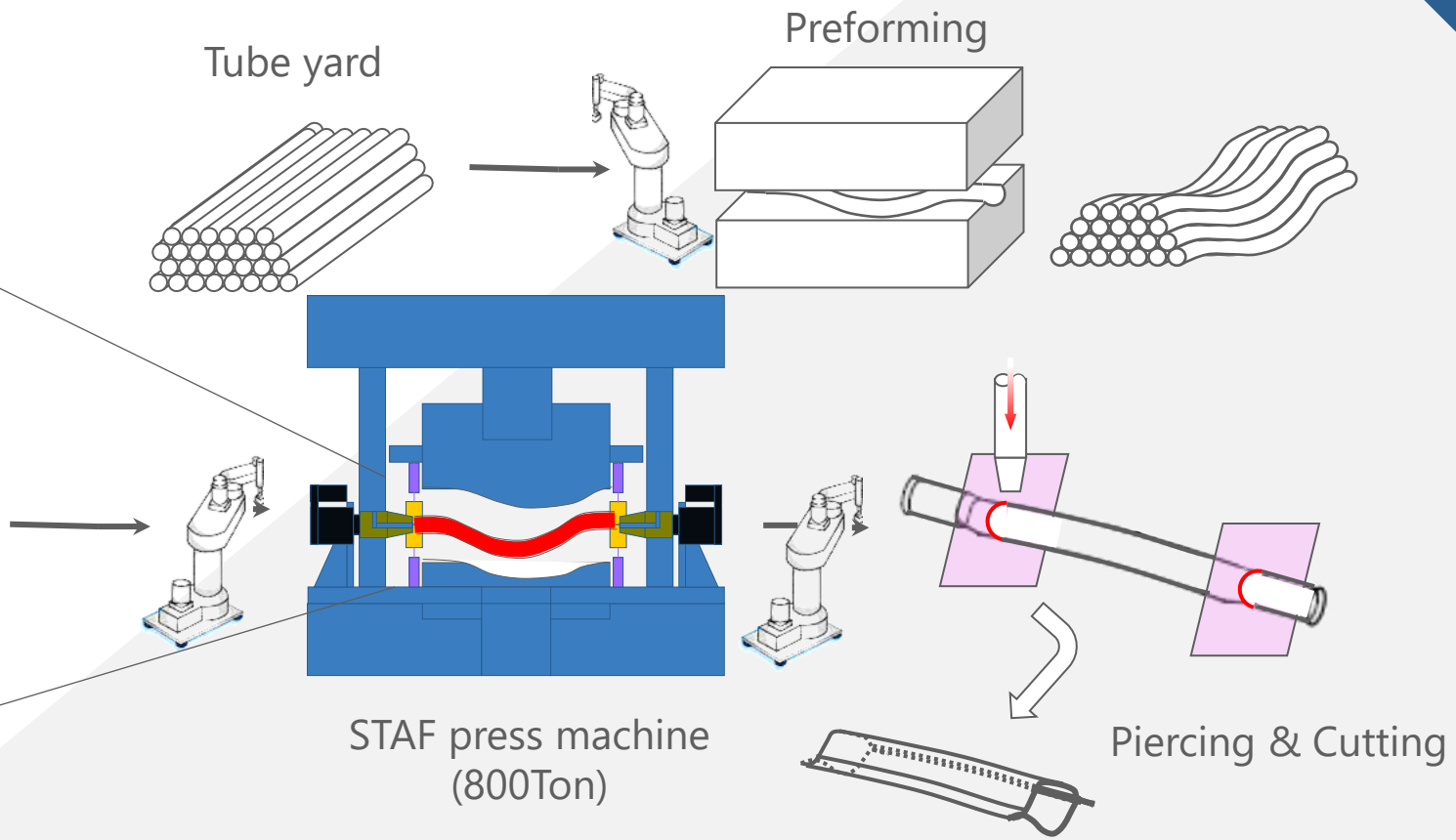

Why STAF® *Steel Tube Air Forming* ?

GDIS

1. Drastic weight reduction; Improved basic performance

■ Drop weight test

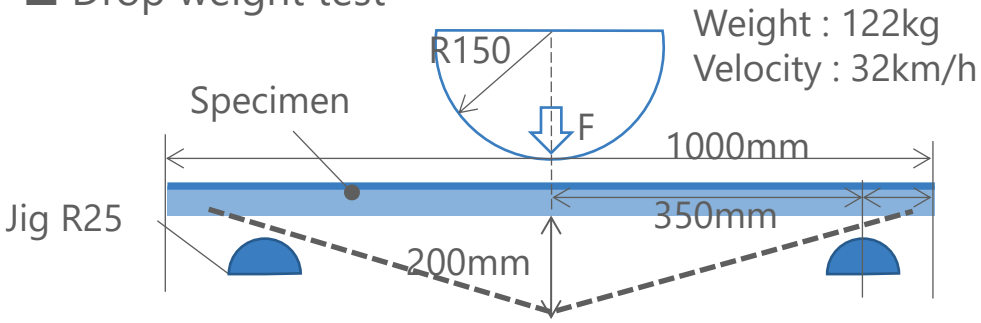

■ Specimen's cross section

■ Actual test result

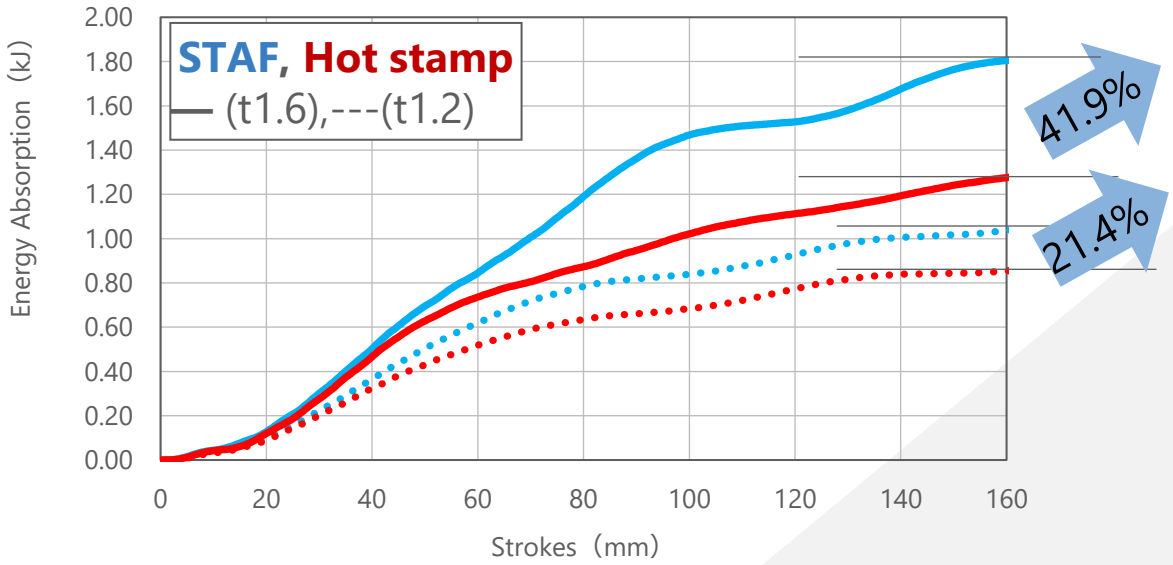

■ After collision

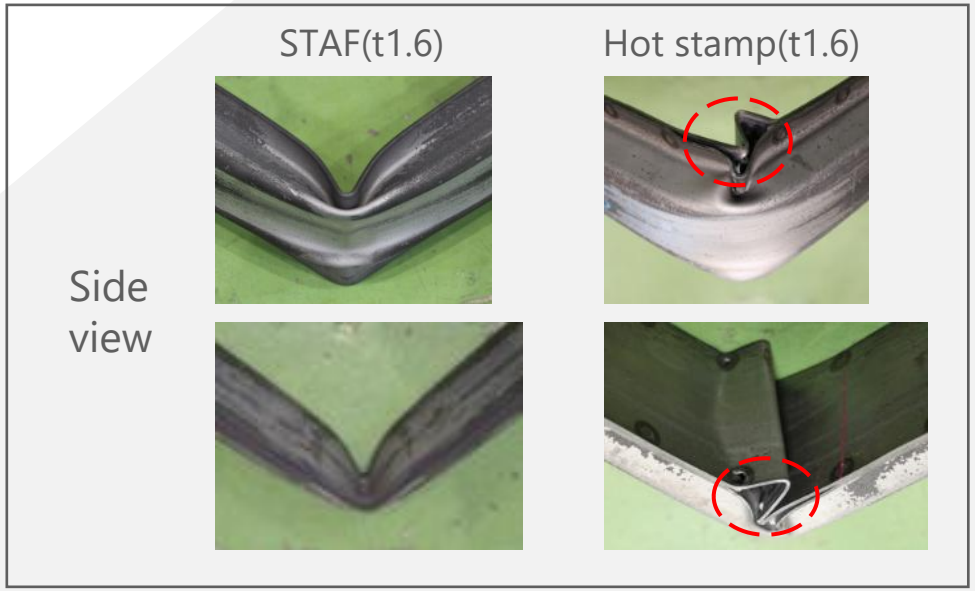

Why STAF® *Steel Tube Air Forming* ?

GDIS

2. Design Flexibility;
   STAF features varying sections which align with design requirements.

- Part integration
- Buckling control
- Tailored section optimization

View Image

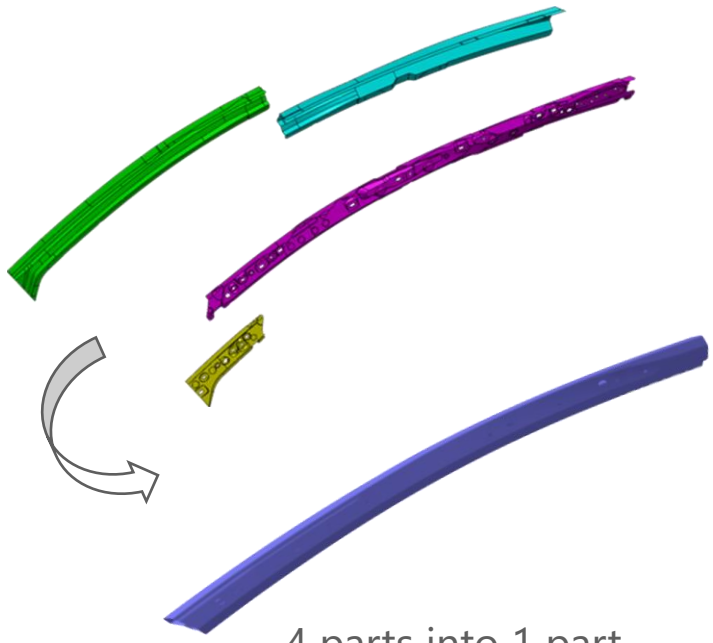

4 parts into 1 part

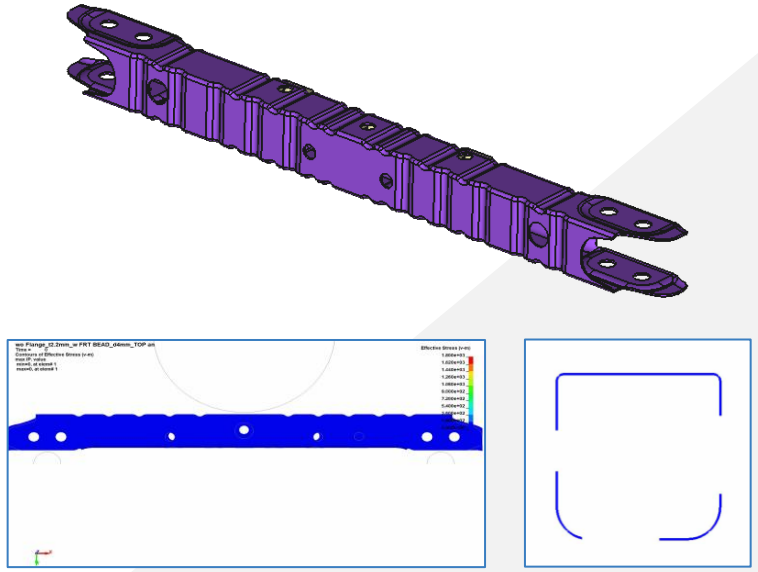

Beam with repeated buckling behavior

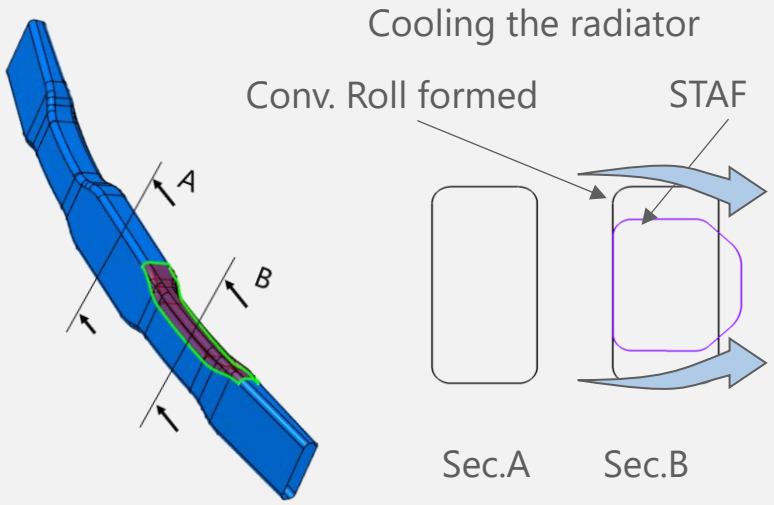

Optimized section for each location

Why STAF® *Steel Tube Air Forming* ?

GDIS

3. Cost reduction; Simplified structure and compact & ecofriendly equipment

	Hydroforming	Hot stamping	**STAF**	Hot gas forming
Strength	~980MPa	**1,500MPa~**	**1,500MPa~**	**1,500MPa~**
Parts construction	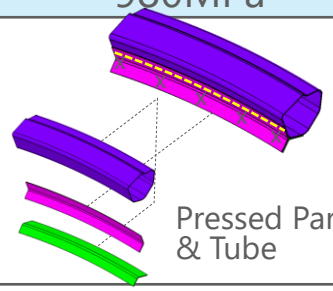	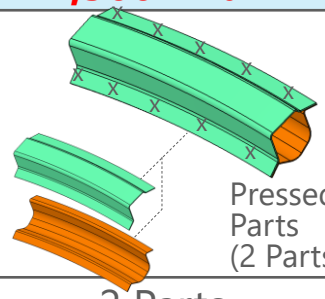	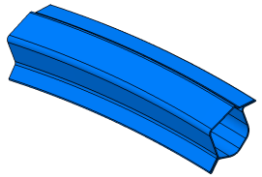	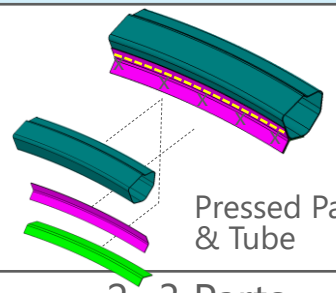
	2~3 Parts	2 Parts	**1 Part**	2~3 Parts
Cross section image	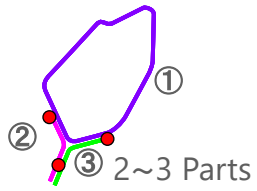	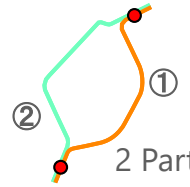	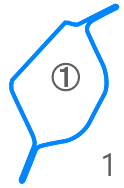	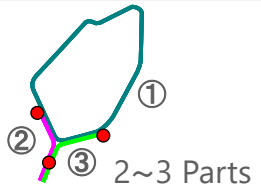
Process	5 processes	5 processes	**3 processes**	6 process
	➢ Preforming ➢ Hydroforming (3000Ton~) ➢ Laser cutting ➢ Press forming ➢ Welding(ass'y)	➢ Blanking ➢ Heating furnace ➢ Hot stamping (2 Sheets &2 Dies) ➢ Laser cutting ➢ Welding(ass'y)	➢ Preforming ➢ STAF(800Ton~) ➢ Laser cutting	➢ Preforming ➢ Heating furnace ➢ Gas forming ➢ Laser cutting ➢ Press forming ➢ Welding(ass'y)

Multi-Forming Structures (MFS); A STAF-Centered Space-Frame Architecture

GDIS

Multi-Forming Structures (MFS):

A vehicle structural concept based on a multi-forming philosophy, **with STAF as the key structural frame** and complementary processes applied where beneficial.

Limitation of Conventional Monocoque

- Interrupted load paths
- Potential weld-joint separation under impact

Key Attributes

- Space-frame stiffness within monocoque packaging
- Continuous Tubular Load Paths
- Lightweighting
- Part Consolidation by STAF

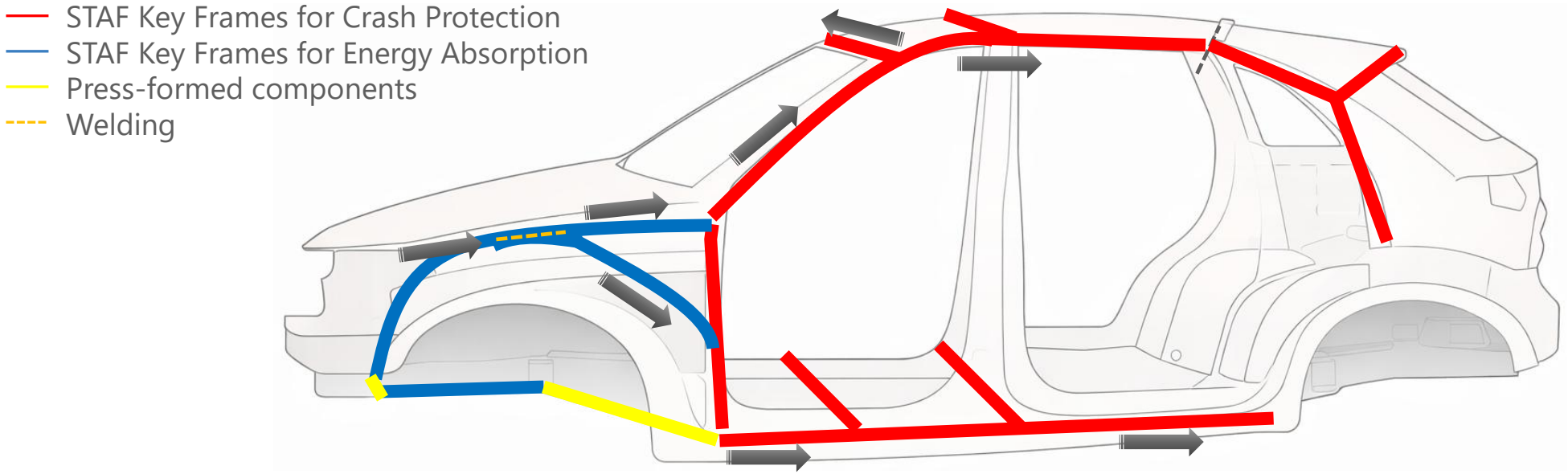

Key Features of MFS

Continuous Load Path

Distributed tubular load paths improve global stiffness

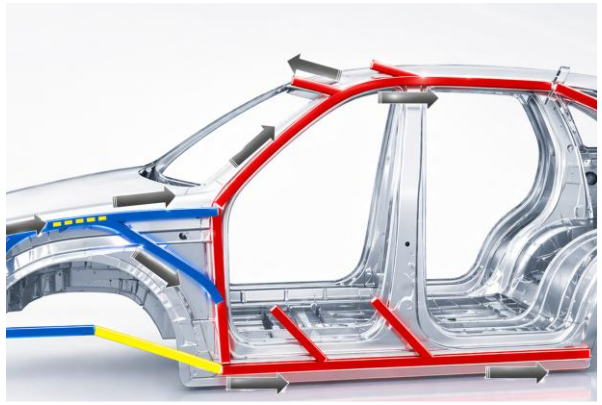

Continuous Tubular Door & Roof Ring

Continuous tubular members create a rigid occupant safety and enhance side-impact resistance through closed-loop load transfer

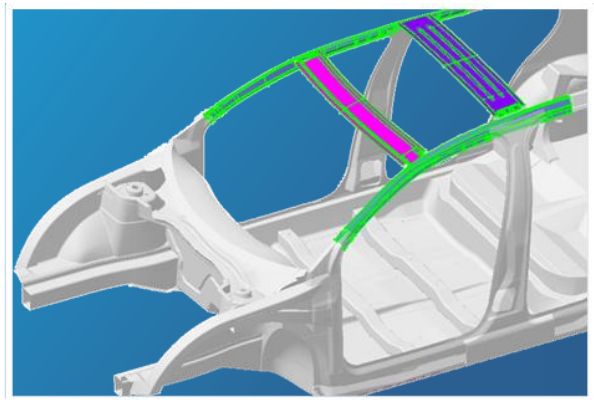

Front Truss Structure

Truss STAF members absorb front crash energy while forming efficient structural load paths toward the cabin.

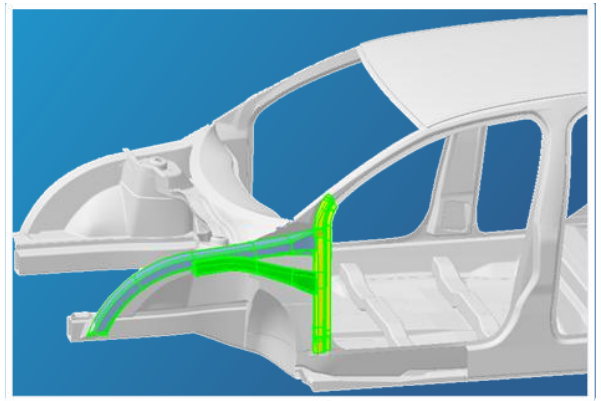

Ultra-Compression Flanged-Beam

Weld-free flanges are ideal for side-impact protection, optimizing safety for both occupants and the battery.

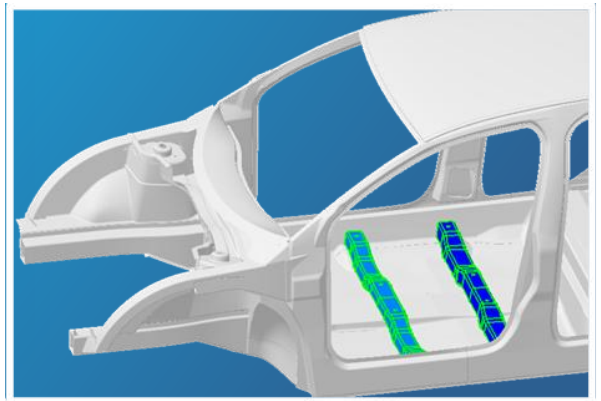

Continuous STAF flanges enhance structural strength.

Integrated flanges reduce part count through part consolidation.

Flanges also simplify assembly by reducing joining brackets.

Key Features of MFS

GDIS

Distinctive A-pillar design

MFS A Pillar Key Innovation

- Hybrid A-Pillar's flange structure
  - Double-flange front for strength and visibility
  - Single-flange rear for stiffness efficiency
- Unique geometry enabling 2-part integration into 1

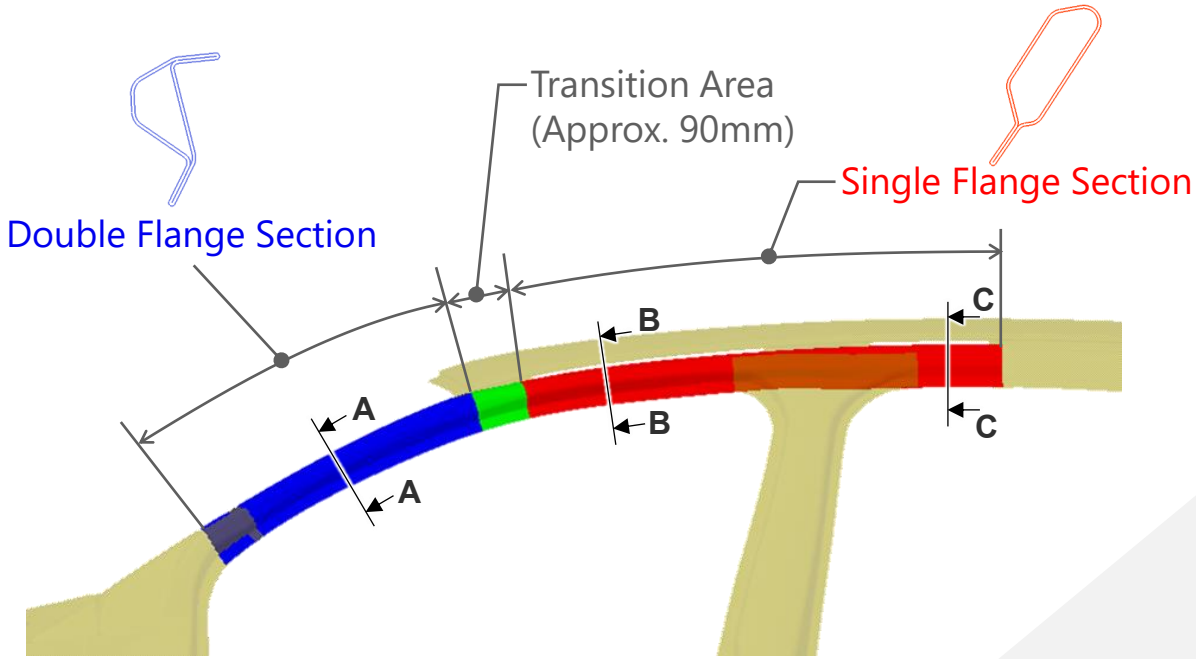

MFS A pillar(φ60.5mm/t1.4mm) vs. Baseline (OTR /t1.8㎜、INR/t1.5mm)
Perimeter range: 189.97~195.6mm (100~103%)
Spot weld count: reduced by 23 points
Number of parts: reduced from 2 to 1

	AA	BB	CC
Baseline Hot Stamp	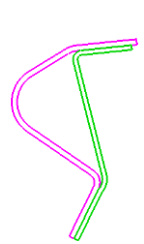	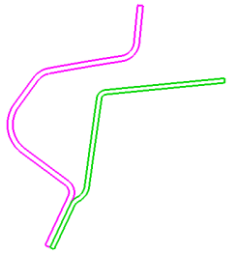	
General STAF CONCEPT (ø60.5mm)	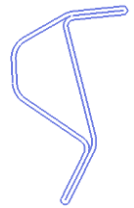	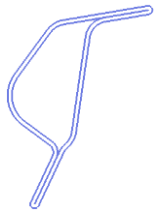	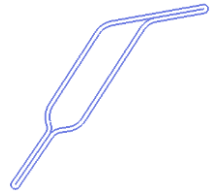
Inertia Matrix	IoyG: 108,400mm4	IoyG: 110,200mm4	IoyG: 127,300mm4
STAF NEW Concept (ø60.5mm)	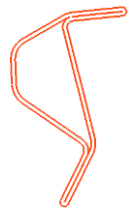	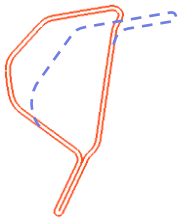	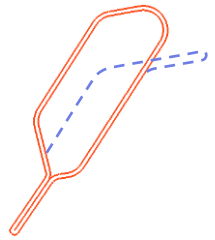
Inertia Matrix	IoyG: 108,400mm4	IoyG: 113,900mm4	IoyG: 155,100mm4

Patent Pending by Sumitomo Heavy Industries, Ltd

Key Features of MFS

GDIS

CAE Evaluation for A pillar

■ Full-Frontal compression test(CAE)
Solver：LS-DYNA
Methods：Forcibly the contact area is moved at 0.5 mm/sec.
*The contact area is set as the rigid.

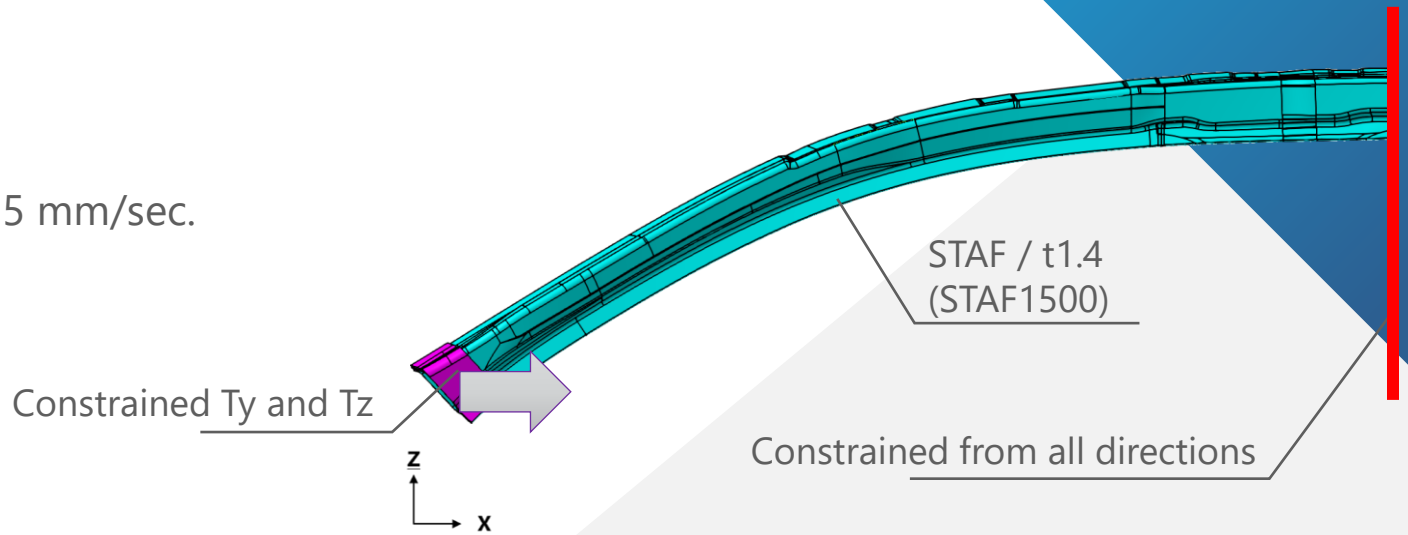

■ Comparison Models

Baseline model A pillar(1500MPa)

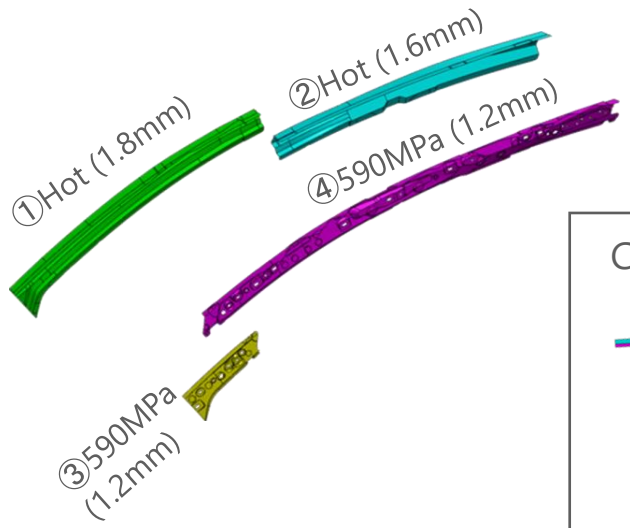

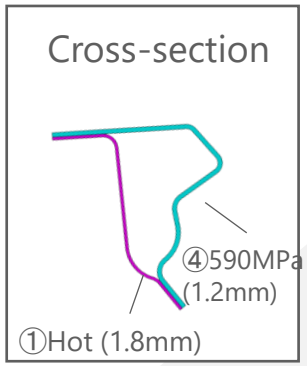

STAF A pillar(1500MPa)

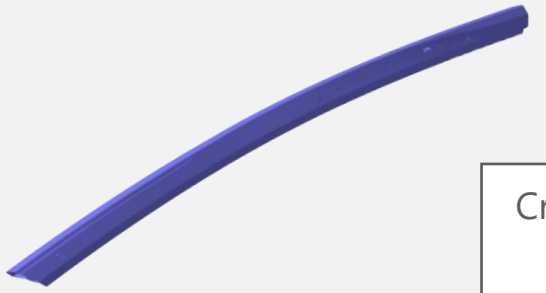

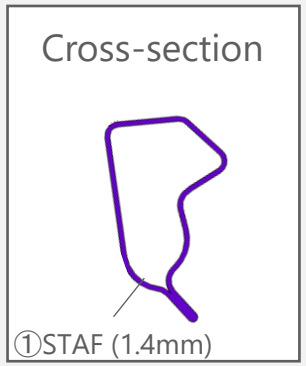

Key Features of MFS

GDIS

Analysis Results

■ Test Result

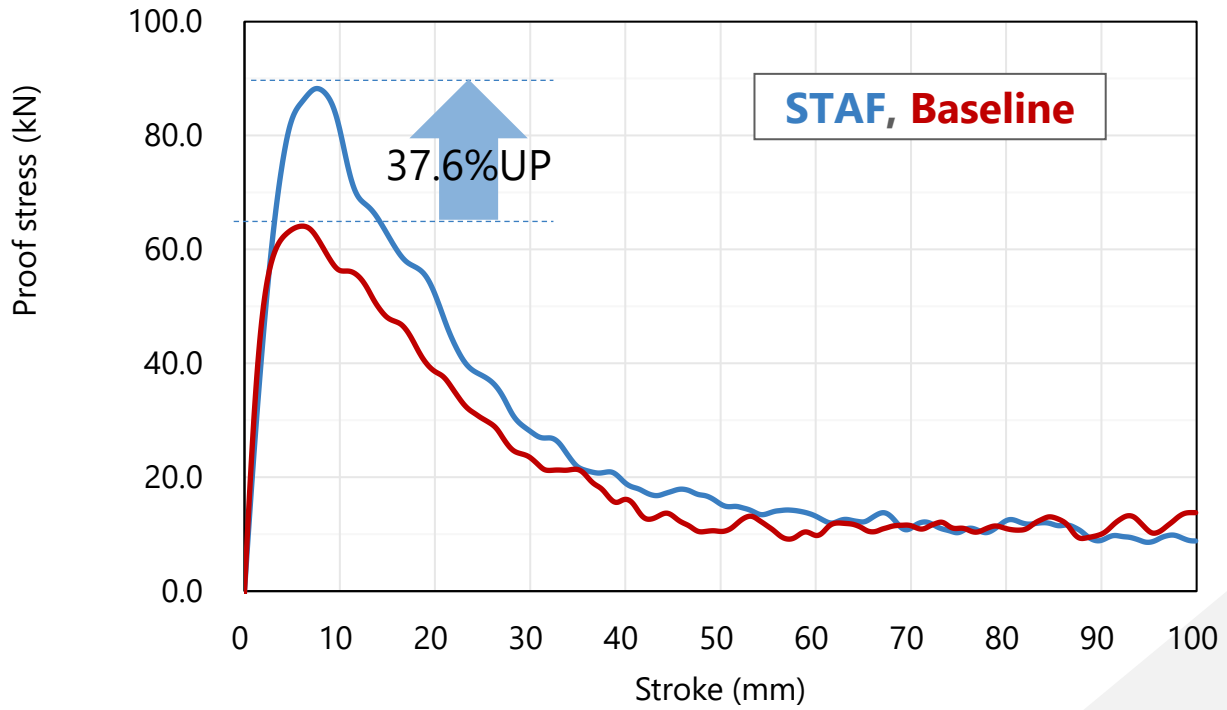

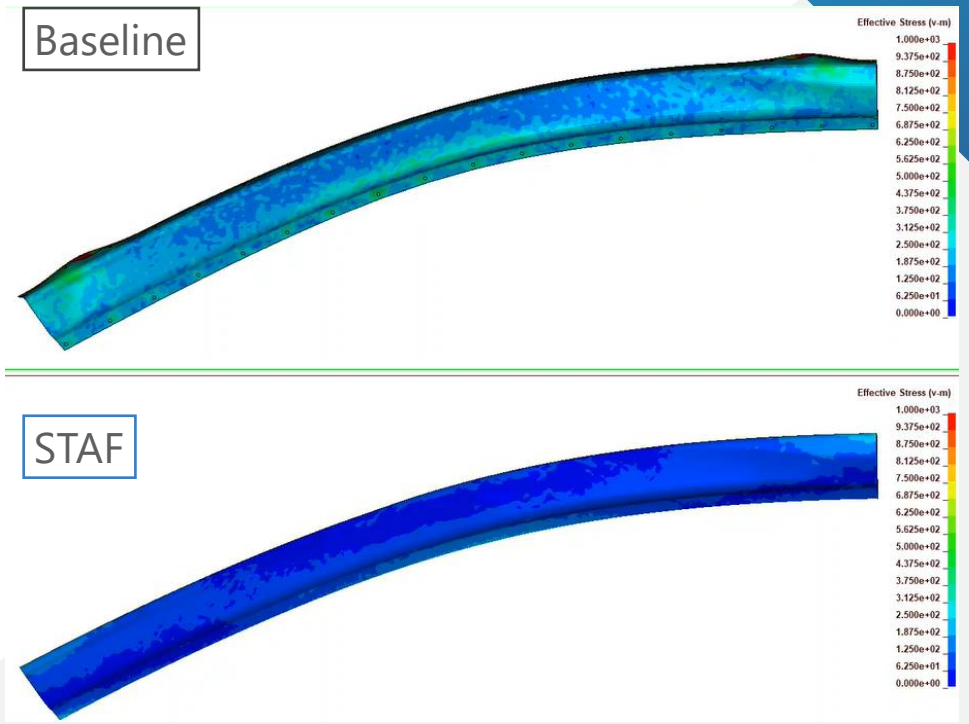

	STAF		Market model
Parts count	1 part	⇩Reduce 3 parts	4 parts
Weight	3.8kg	⇩31% Weight reduction	5.5kg

CAE Validation of MFS Vehicle Concept

GDIS

- An existing vehicle (Model A) was used, and 15 key structural components were re-engineered based on the MFS.
- By reducing the gauge in the STAF components and their related surrounding parts to achieve equivalent performance, body-in-white mass was reduced from 292 kg in the baseline vehicle to 262 kg with the STAF application.

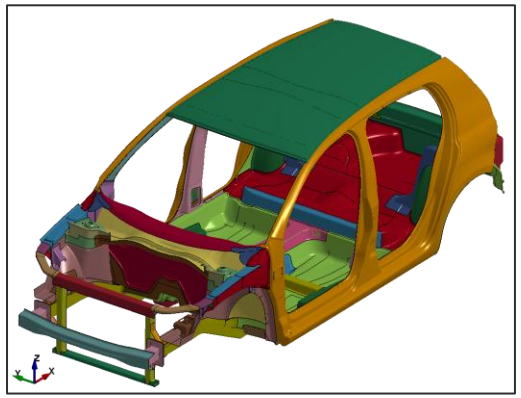

Baseline Steel Based
Global Standard Vehicle

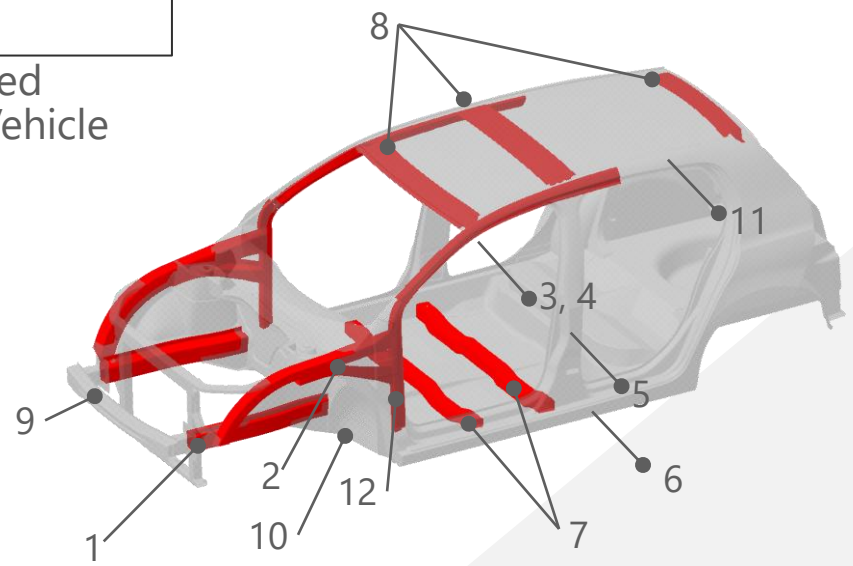

MFS Concept

Replaced Unreplaced

	Key MFS Frames		
No.	Frame Name	Baseline Material Grade	MFS Concept Material Grade
1	Front Side Frame	HSS	STAF TS980*
2	Upper Member	AHSS	STAF TS980*
3	Front Pillar (A-Pillar)	UHSS	STAF TS1500
4	Roof Side Rail	UHSS	STAF TS1500
5	Center Pillar (B-Pillar)	UHSS	
6	Side Sill	UHSS	
7	Floor Cross Member	AHSS	STAF TS 1500
8	Roof Member Front	AHSS	STAF TS 1500
	Roof Member Center	AHSS	STAF TS 1500
	Roof Member Rear	AHSS	STAF TS 1500
9	Bumper Beam	UHSS	
10	Dashboard Mem.	HSS	HSS
11	C Pillar	AHSS	
12	Hinge Pillar	HSS	STAF TS1500
	Total BiW weight	292.285	262.1(-30.2kg, -10.3%)

*Currently under development

CAE Setup for Vehicle Stiffness Evaluation

GDIS

CAE Setup

1. CAE analysis: Torsional Stiffness

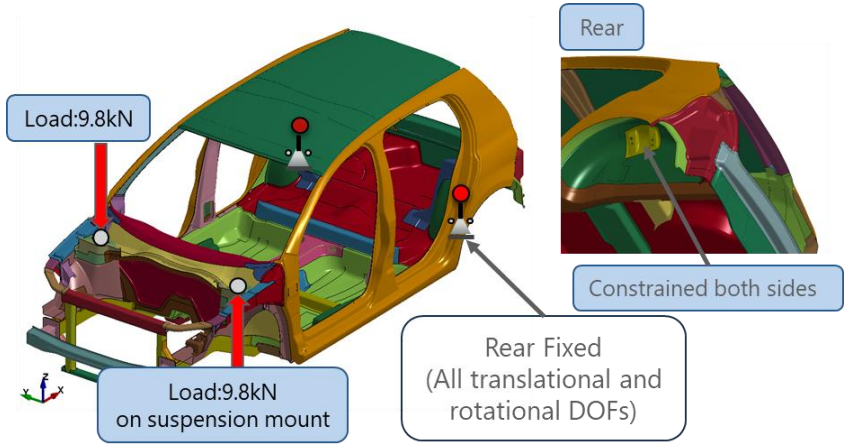

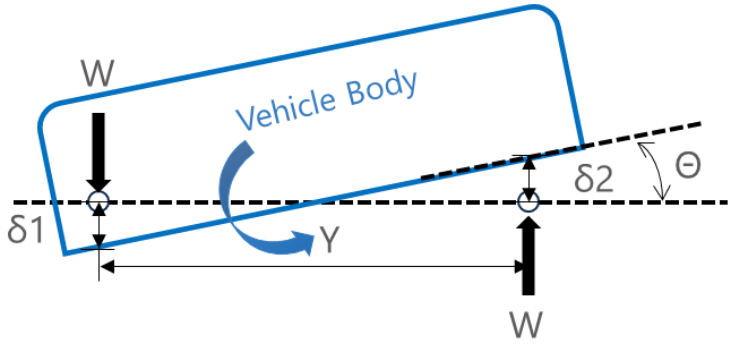

W : Applied Load
δ_1 : Vertical Displacement at Right Load Point
δ_2 : Vertical Displacement at Left Load Point
Y : Distance Between Load Points
θ : Torsion Angle

2. CAE analysis: Bending Stiffness

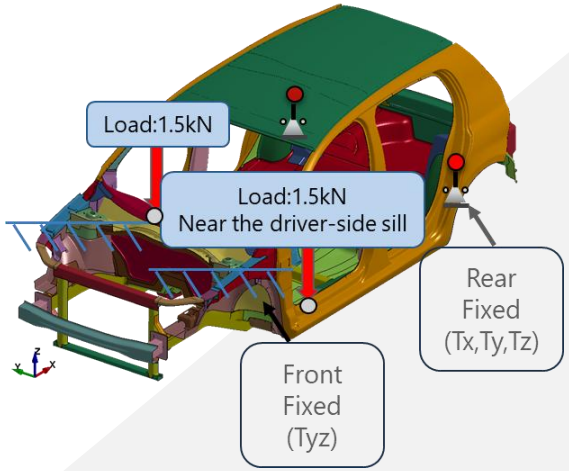

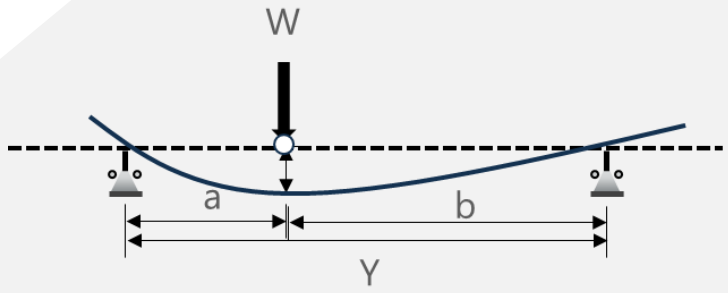

W : Applied Load (at h-point)
L : Span Length (Distance b/w Supports)
a, b : Distance from Supports to Load Point
δ : Vertical Deflection

CAE Validation of MFS; Torsional Stiffness

GDIS

Analysis Results

- STAF MFS vs. Baseline (Model A) Max Z-displacement: STAF MFS: −17.22 / +22.57 mm Baseline: −26.23 / +29.24 mm
  → Superior performance in maximum displacement
- Component displacement: 20–50% reduction observed at key locations: Front support, Seat cross member, A-pillar
  → Consistent improvement across major structural components

1. STAF MFS

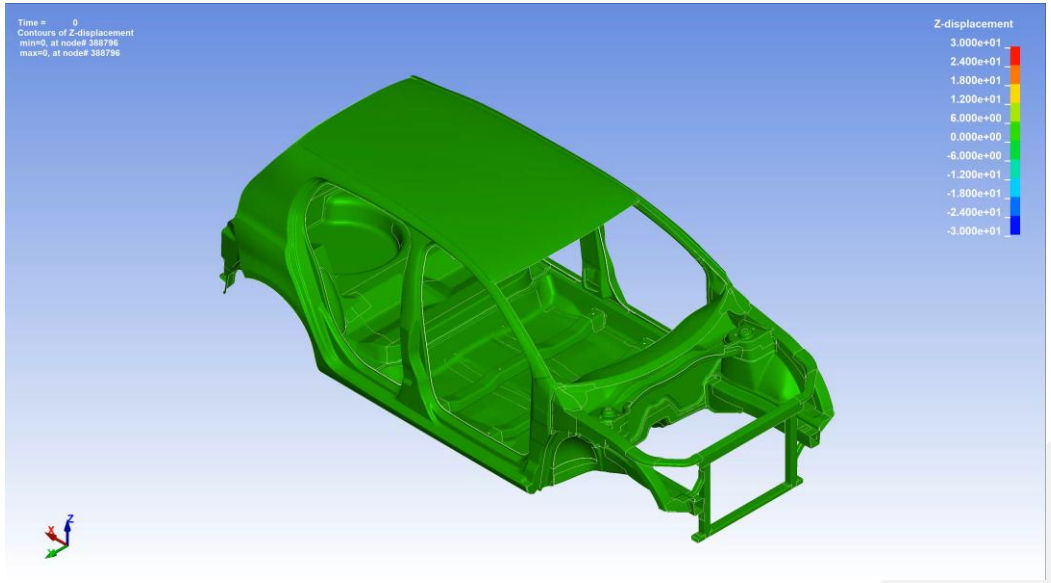

2. Baseline (Model A)

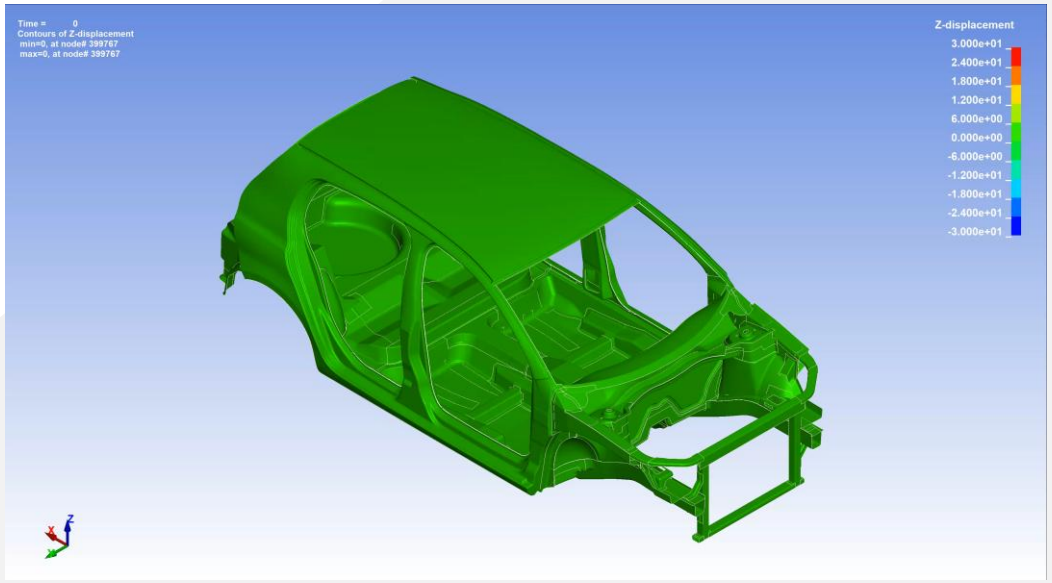

CAE Validation of MFS; Torsional Stiffness

GDIS

Analysis Results

Max Z-Disp. Location

1. STAF MFS

Max Z-Disp: -17.22/+22.57 mm

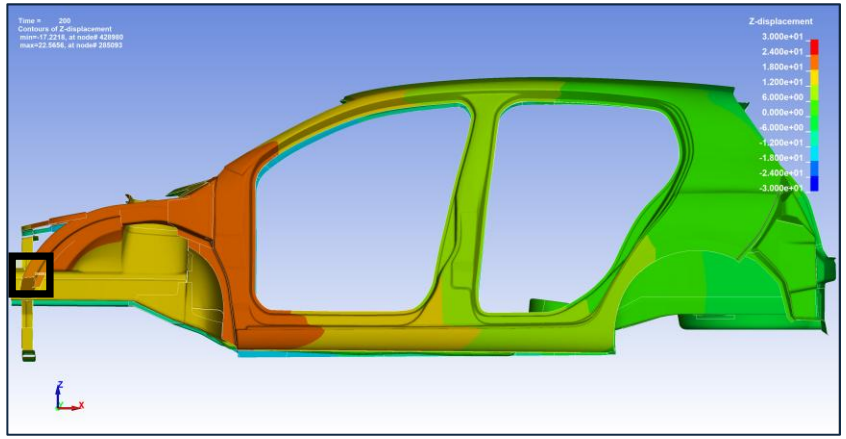

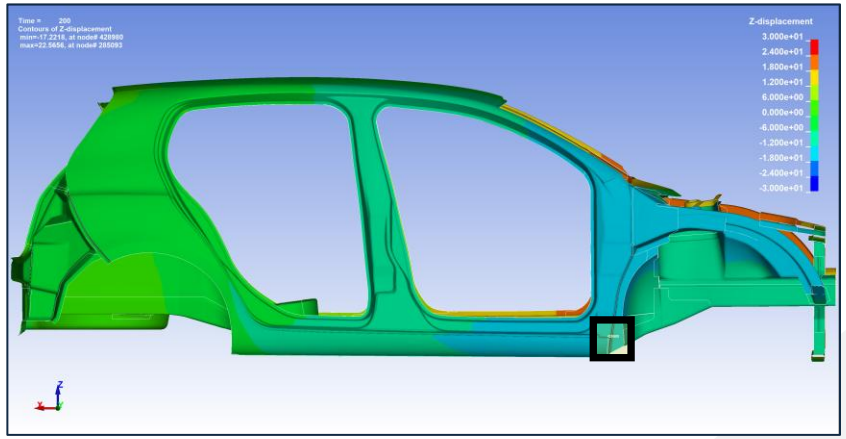

2. Baseline (Model A)

Max Z-Disp: -26.23/+29.24 mm

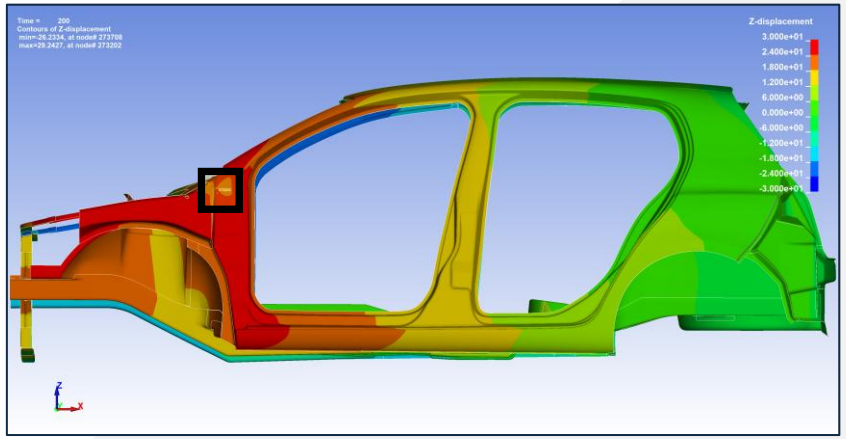

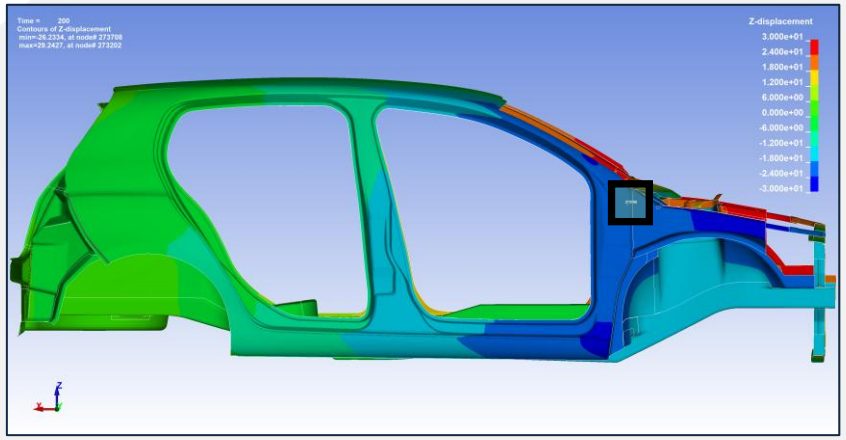

CAE Validation of MFS; Torsional Stiffness

GDIS

Analysis Results

Max Z-Disp. Location

Displacement measurement locations;

Front grille support bracket

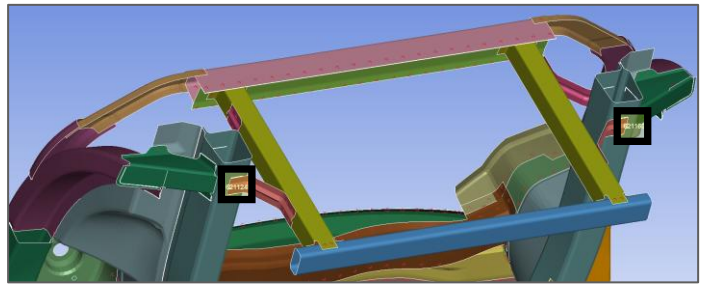

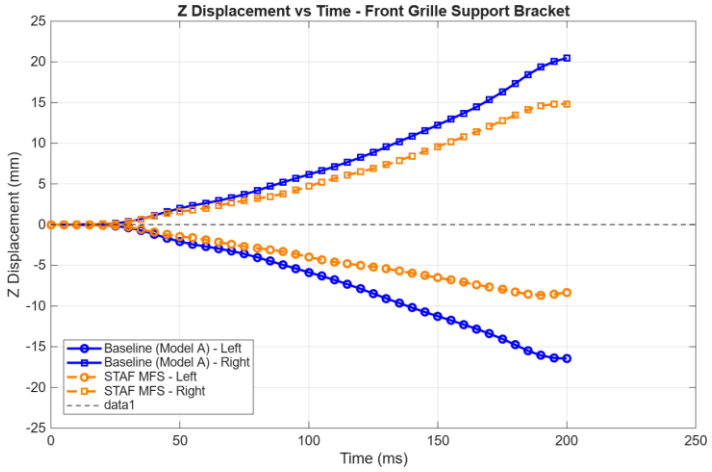

- Reduction in left side: 49.33%
- Reduction in right side: 27.49%

Seat Cross Mem. Support

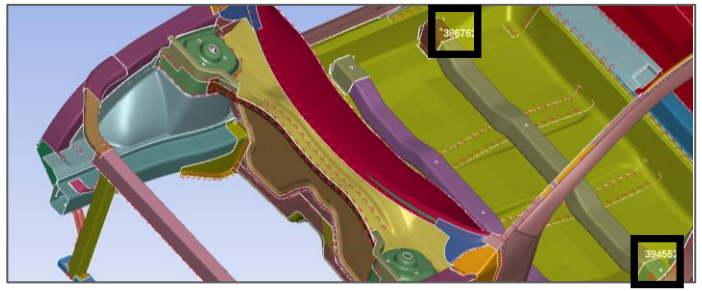

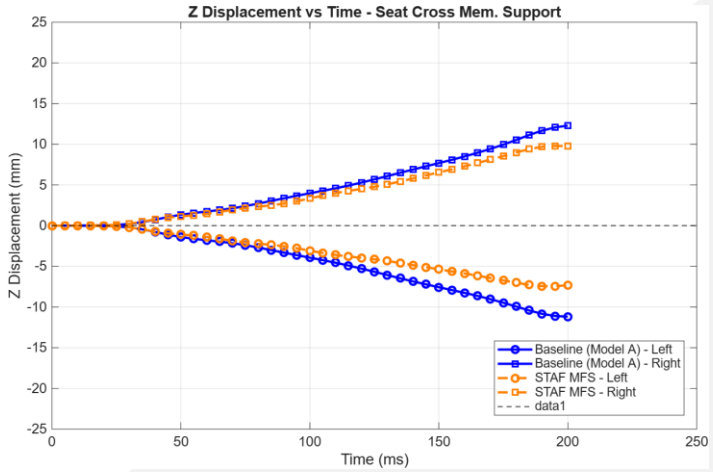

- Reduction in left side: 34.58%
- Reduction in right side: 20.58%

A Pillar INR Center

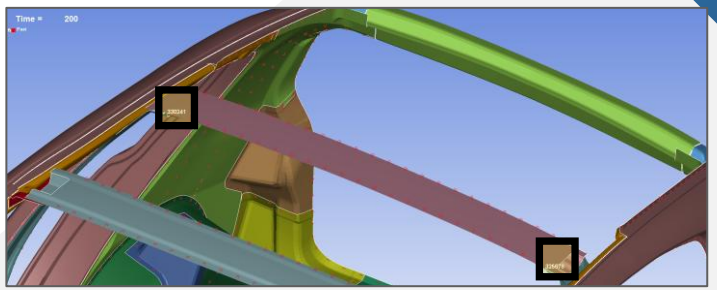

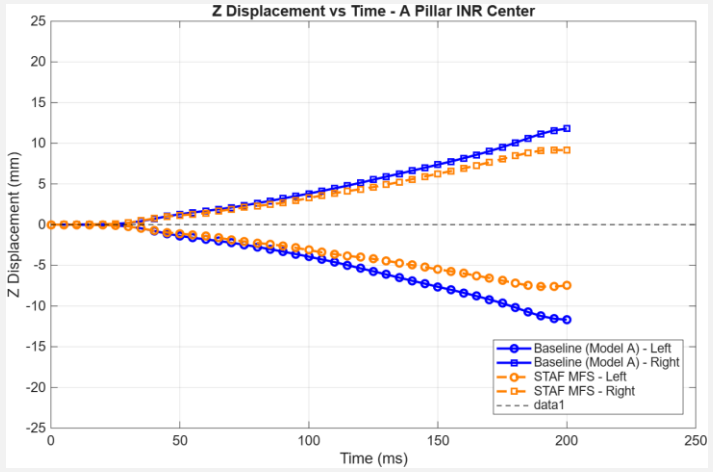

- Reduction in left side: 35.87 %
- Reduction in right side: 22.44 %

CAE Validation of MFS; Torsional Stiffness

GDIS

Analysis Results

- STAF V1 vs. Baseline (Model A) Max. von Mises stress: STAF: 556.6 MPa, Baseline: 600.6 MPa
- Based on the stress distribution, STAF exhibits improved load distribution due to the tubular structure and enhanced sectional performance. This allows the load to be carried more uniformly without generating high local stress concentrations.

1. STAF MFS

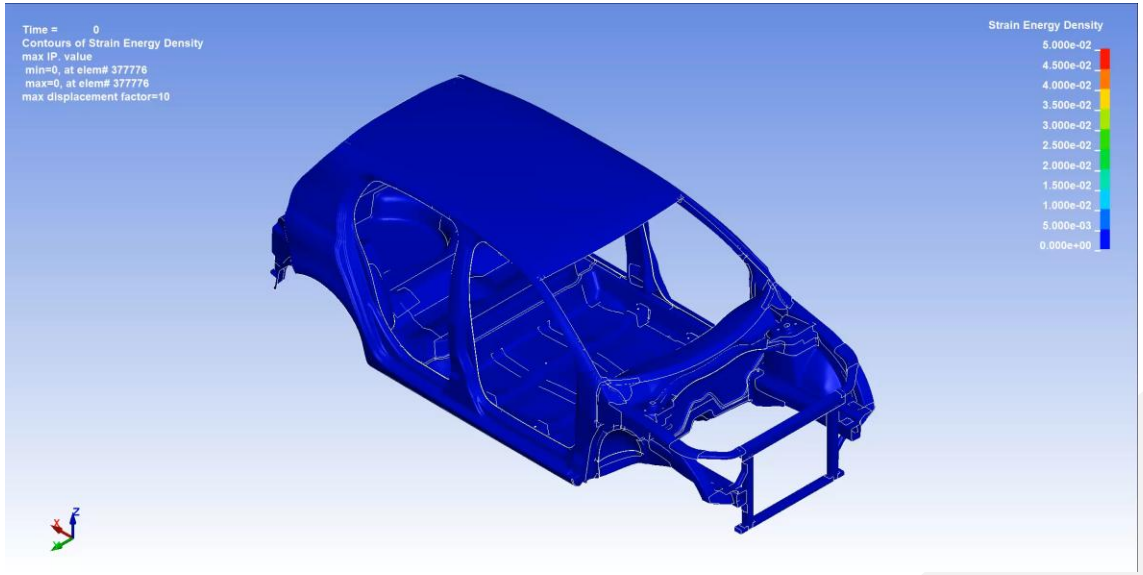

2. Baseline (Model A)

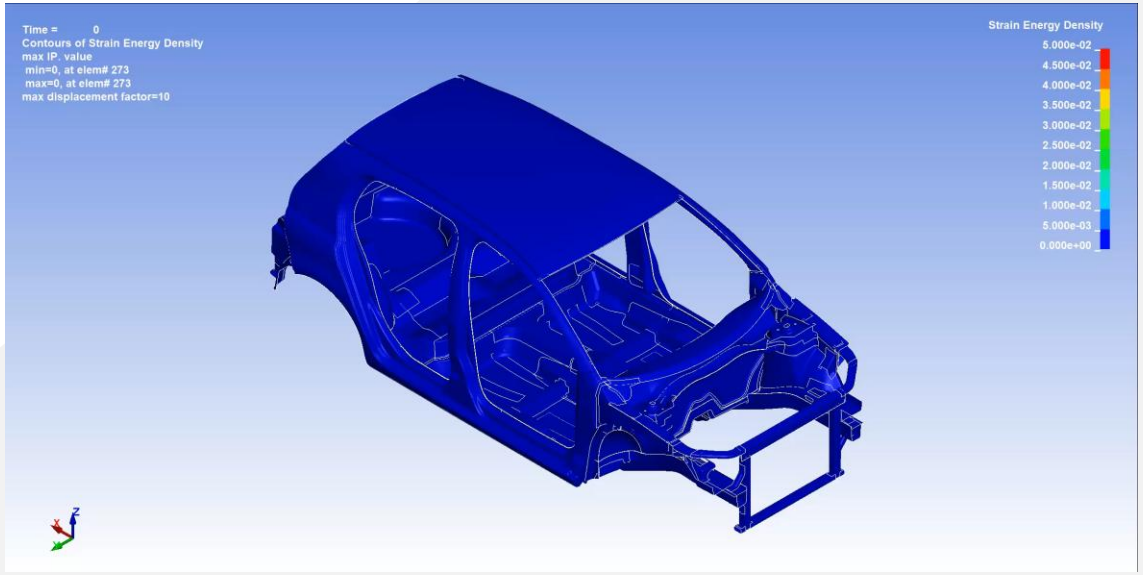

CAE Validation of MFS; Torsional Stiffness

GDIS

Analysis Results

Mechanism of performance improvement

- The Front Truss structure distributes torsional load, reducing strain energy concentration in the front body region.
- The STAF A-pillar structure provides an efficient load path, suppressing localized strain energy accumulation and improving overall torsional stiffness.

1. STAF MFS

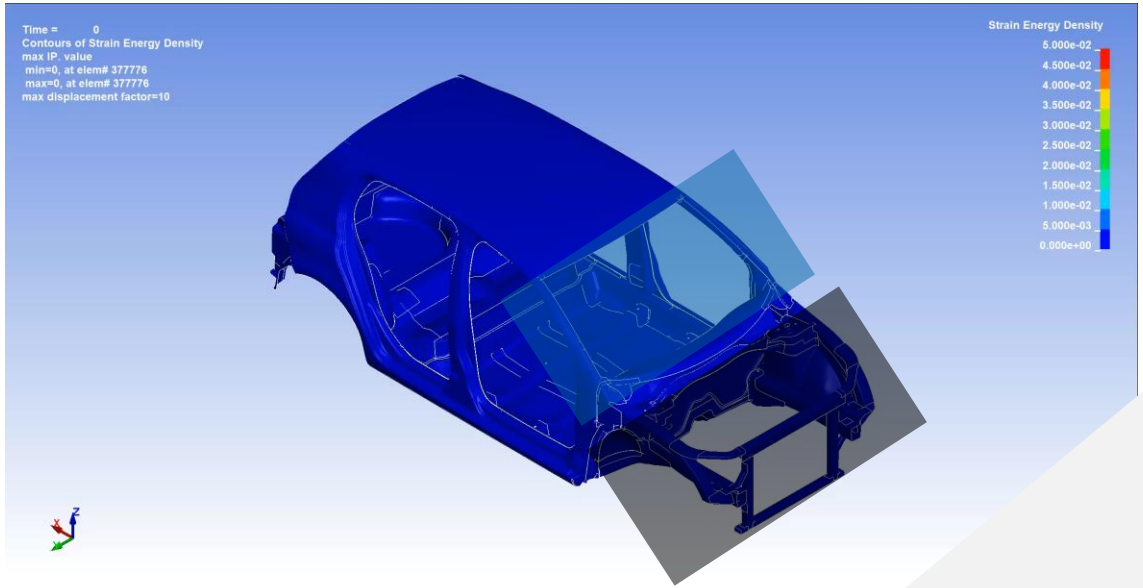

2. Baseline (Model A)

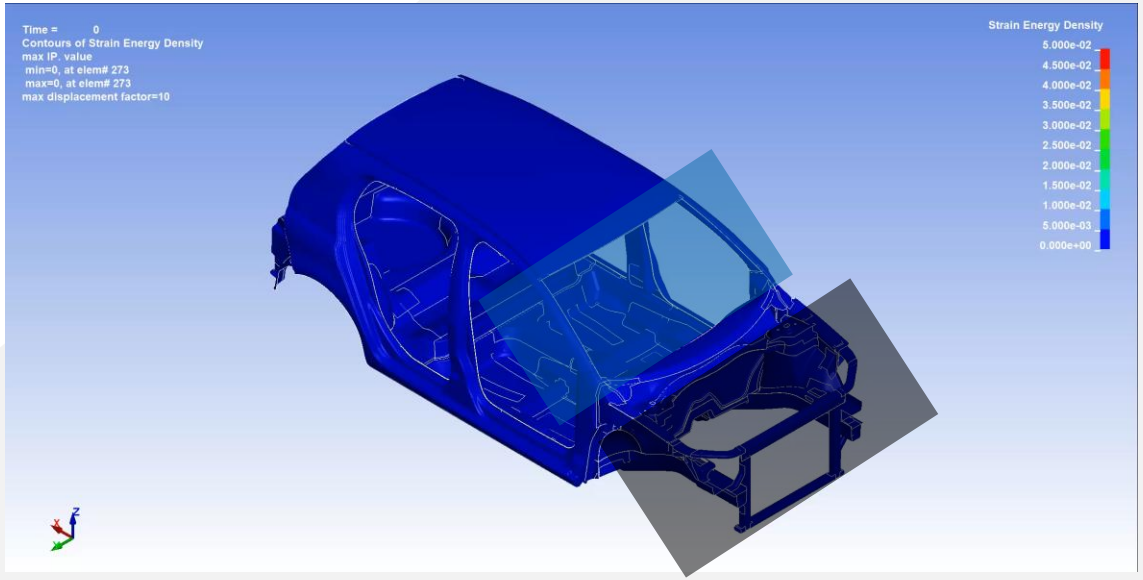

CAE Validation of MFS; Torsional Stiffness

GDIS

Analysis Results

Stress evaluation focused on STAF-related regions

- **Stress Reduction through Improved Load Distribution**
- Peak stress in A-pillar reduced from **400–500 MPa** to **387.5 MPa**
- More uniform load distribution achieved with STAF
- Reduced stress concentration observed across STAF-applied regions

1. STAF MFS A Pillar

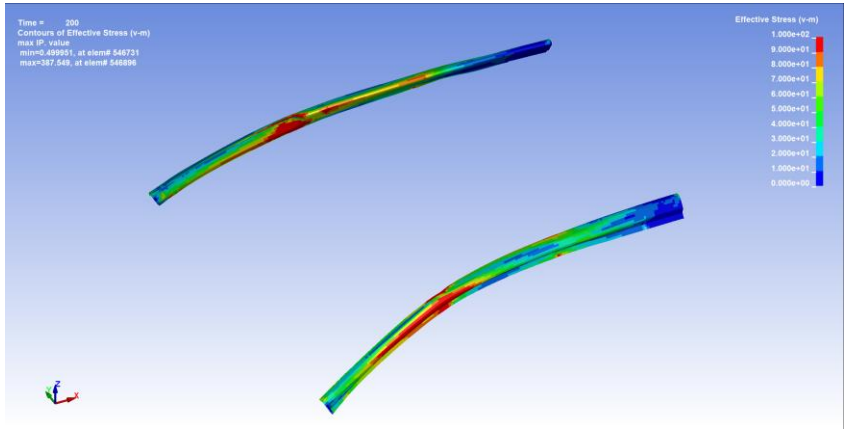

STAF-A Pillar: 387.549 MPa

2. Baseline (Model A) A Pillar OTR, INR

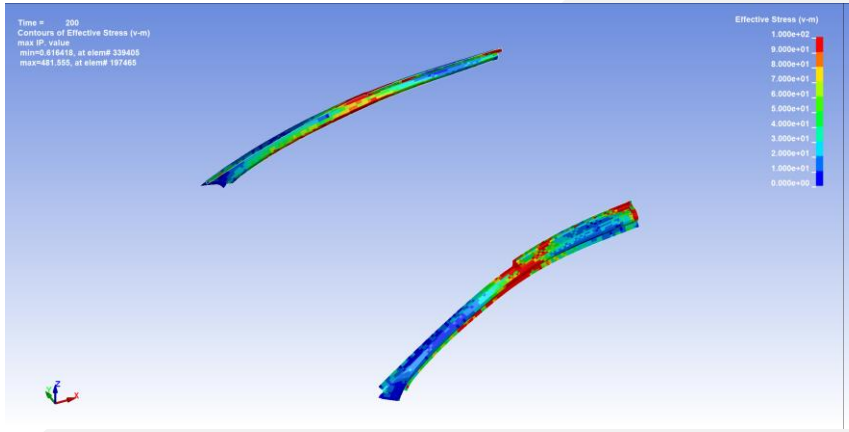

Baseline-A Pillar OTR: 481.555MPa

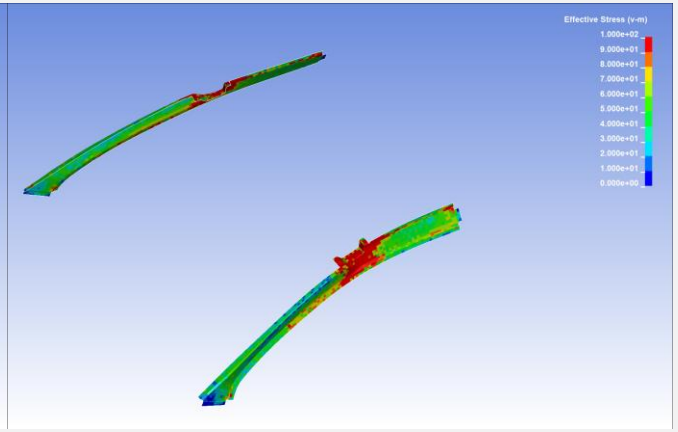

Baseline-A Pillar INR: 409MPa

CAE Validation of MFS; Bending Stiffness

GDIS

Analysis Results

- STAF MFS vs. Baseline (Model A) Max Z-displacement: STAF MFS: -0.82mm, Baseline: -1.26mm(-34.9%)
  → Superior performance in maximum displacement
- Component displacement: Overall deformation reduction was observed at major measurement locations, indicating equivalent structural stiffness performance of the STAF MFS model.

1. STAF MFS

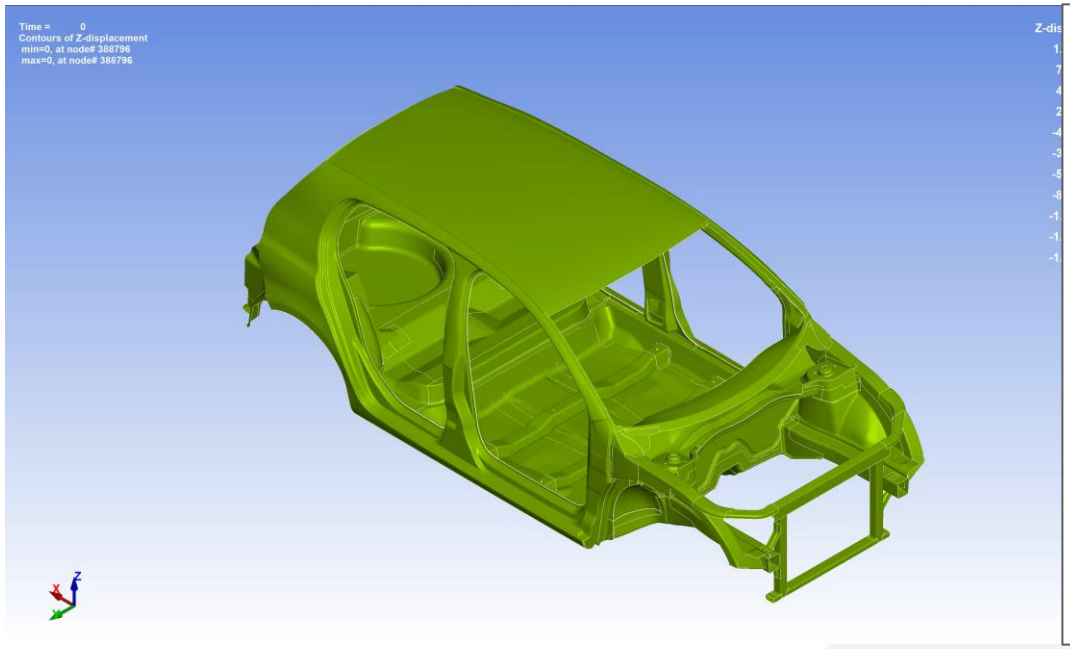

2. Baseline (Model A)

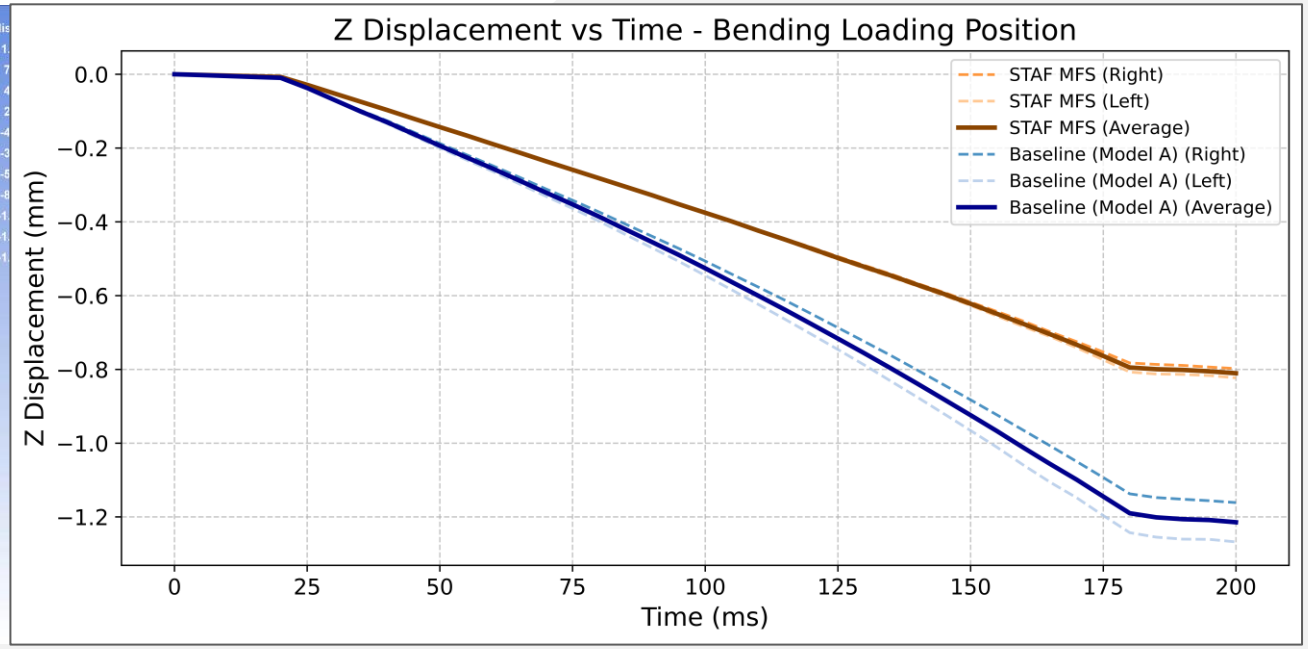

CAE Validation of MFS; Bending Stiffness

GDIS

Analysis Results

Displacement point

Displacement measurement locations;

Front Window Windshield

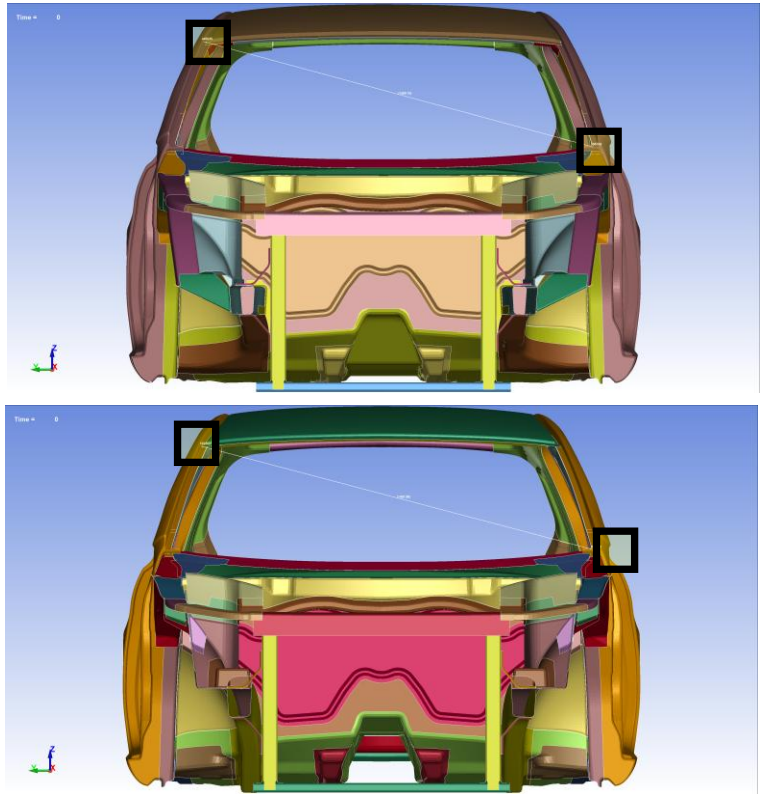

- STAF Deformation: -0.06mm
- Baseline: -0.15mm

Left Front Door

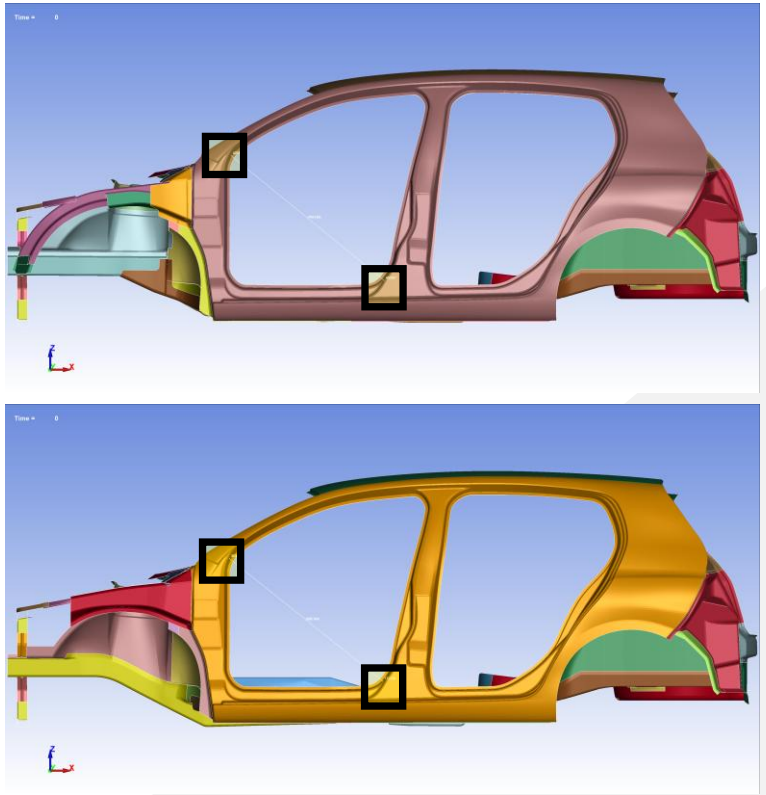

- STAF Deformation: 0.08mm
- Baseline: 0.05mm

Right Front Door

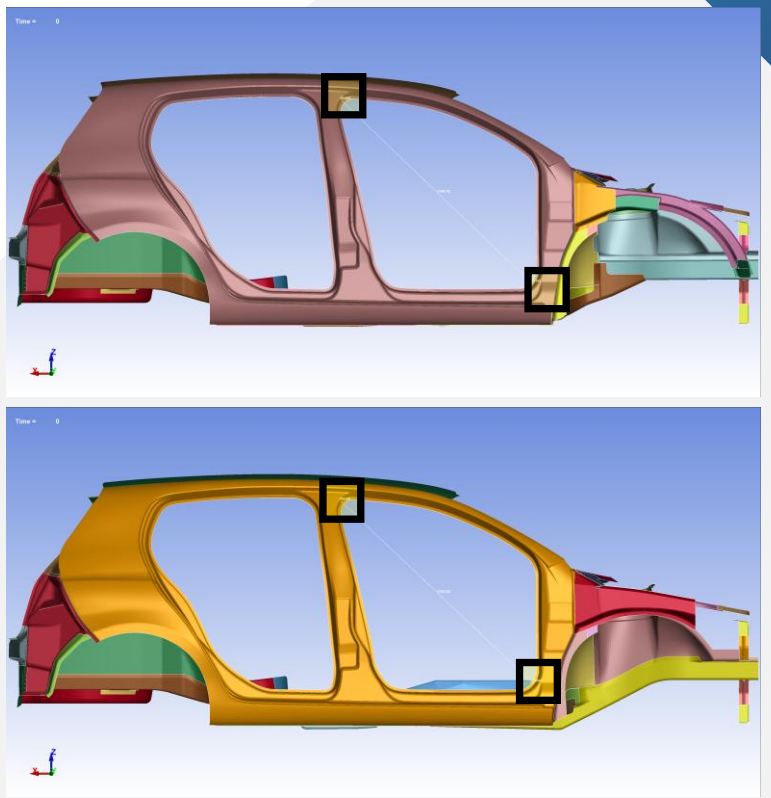

- STAF Deformation: -0.01mm
- Baseline: 0.06mm

Benefits of Mass Reduction

GDIS

Analysis Results

	Baseline	STAF MFS	Improvement
BiW Weight	292.3 kg	262.1 kg	**-30.2 kg (-10.3%)**
Torsional Displacement (Loaded point)	-26.23 / +29.24 mm	-17.22 / +22.57 mm	**23–34% lower**
Component Displacement (Torsion)	100%	20–50%	**50–80% reduction**
Bending Displacement (Loaded point)	-1.26 mm	-0.82 mm	**34.9% lower**
Component Displacement (Bending)	Ave.0.09mm	Ave.0.05mm	Comparable overall

- Despite significant lightweighting, the MFS architecture exceeded conventional performance in torsional and bending stiffness evaluations.

- This demonstrates that the Front Truss Structure enhances global load-path efficiency, while the distinctive MFS A-Pillar provides component-level structural advantages. Their combination establishes superiority at both the vehicle structural level and the component level.

Benefits on Lowering CO2 emissions

GDIS

- STAF dramatically reduces part count compared to conventional monocoque structures.
- As shown below, components like the A-pillar, roof, seat cross member, and front structure are simplified from multiple parts into single integrated parts, enabling a much cleaner and more efficient body design.

Front

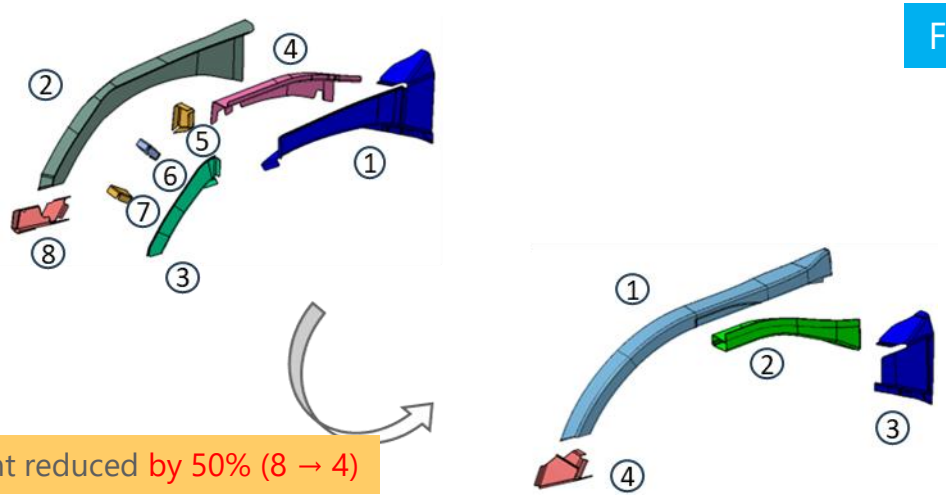

Part count reduced by 50% (8 → 4)

Body Side

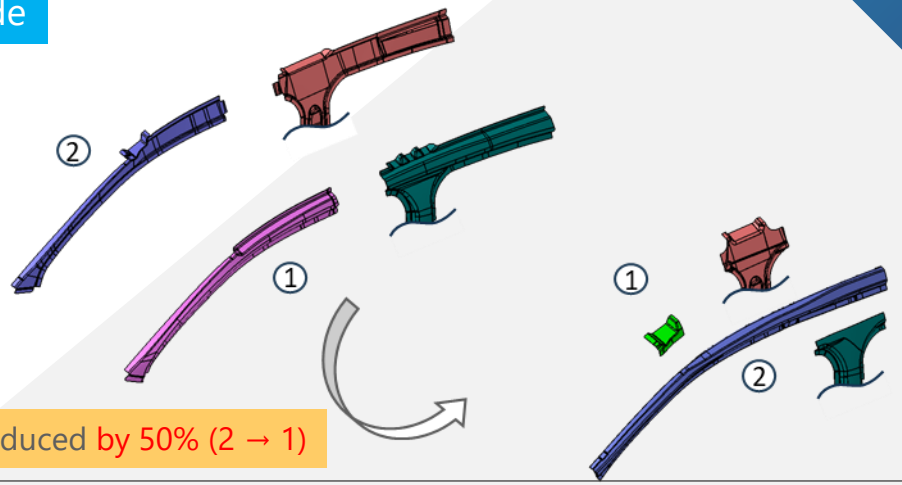

Part count reduced by 50% (2 → 1)

Roof

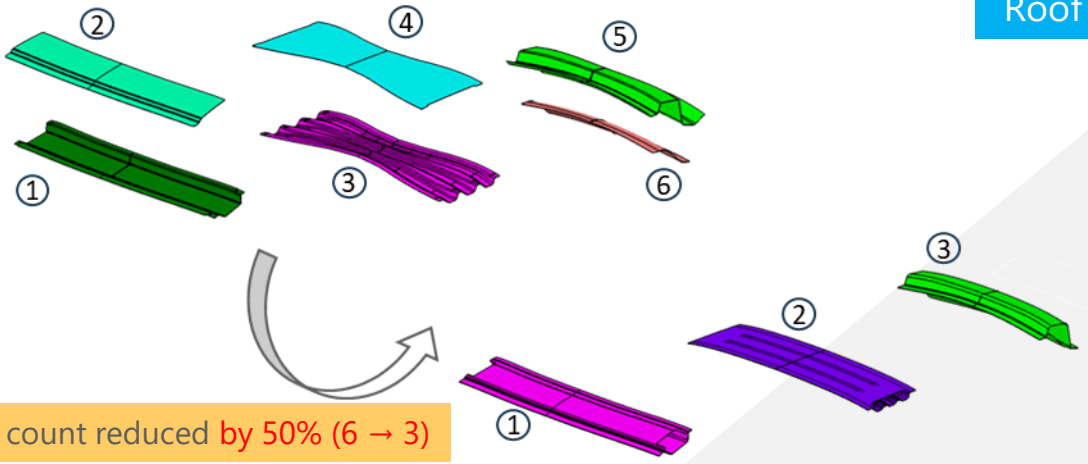

Part count reduced by 50% (6 → 3)

Floor

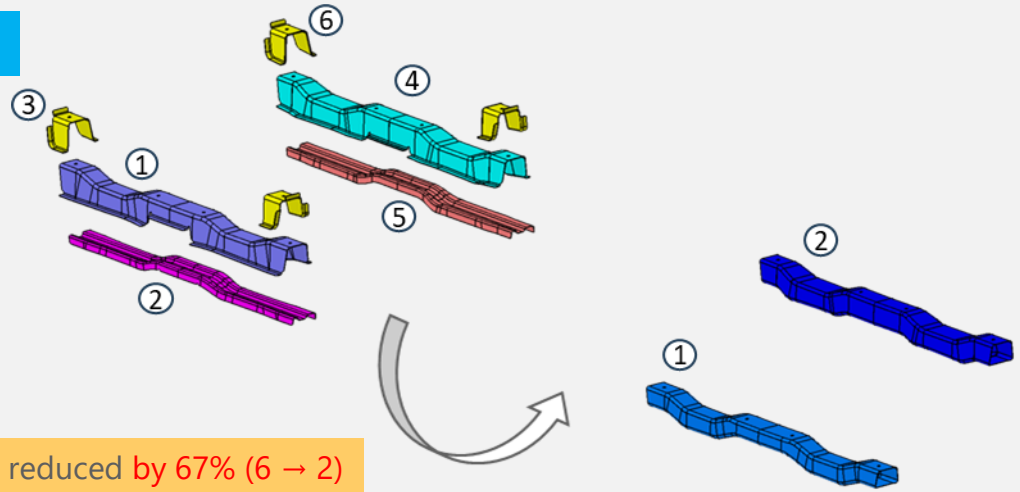

Part count reduced by 67% (6 → 2)

Benefits on Lowering CO2 emissions

GDIS

❑ CO_2 Emissions Calculation Logic for Die Manufacturing

CO2total = CO2material + CO2melting + CO2casting_others + CO2processing + CO2heat

Items	EF; Effective Factor		Unit
Material; Mmetal = Wdie-material x EF	Worldsteel Ave.	1.92	kg-CO2/kg
Melting; Mmelt= Wdie-before melting x EF	Iron induction	0.34	kg-CO2/kg
Casting and Others; Casting and others = CO2melting × 49.5 / 50.5 CO2 ratio Mmelt(50.5%) : Mcasting others(49.5%)			
Processing; Emachining x EFelectricity	US avg electricity	0.37	kg-CO2/kwh
Heat Treatment / Furnace Gas (CO_2 Emission Factor)	Natural gas	0.0503	kg-CO2/MJ
CO2heat [kg] = Mass [kg] × Cp [kJ/kg·K] × ΔT [K] ÷ 1000 × EFgas [kg-CO2/MJ] ÷ ηfurnace	η_furnace =	0.7	

CO2 Emissions Calculation Results

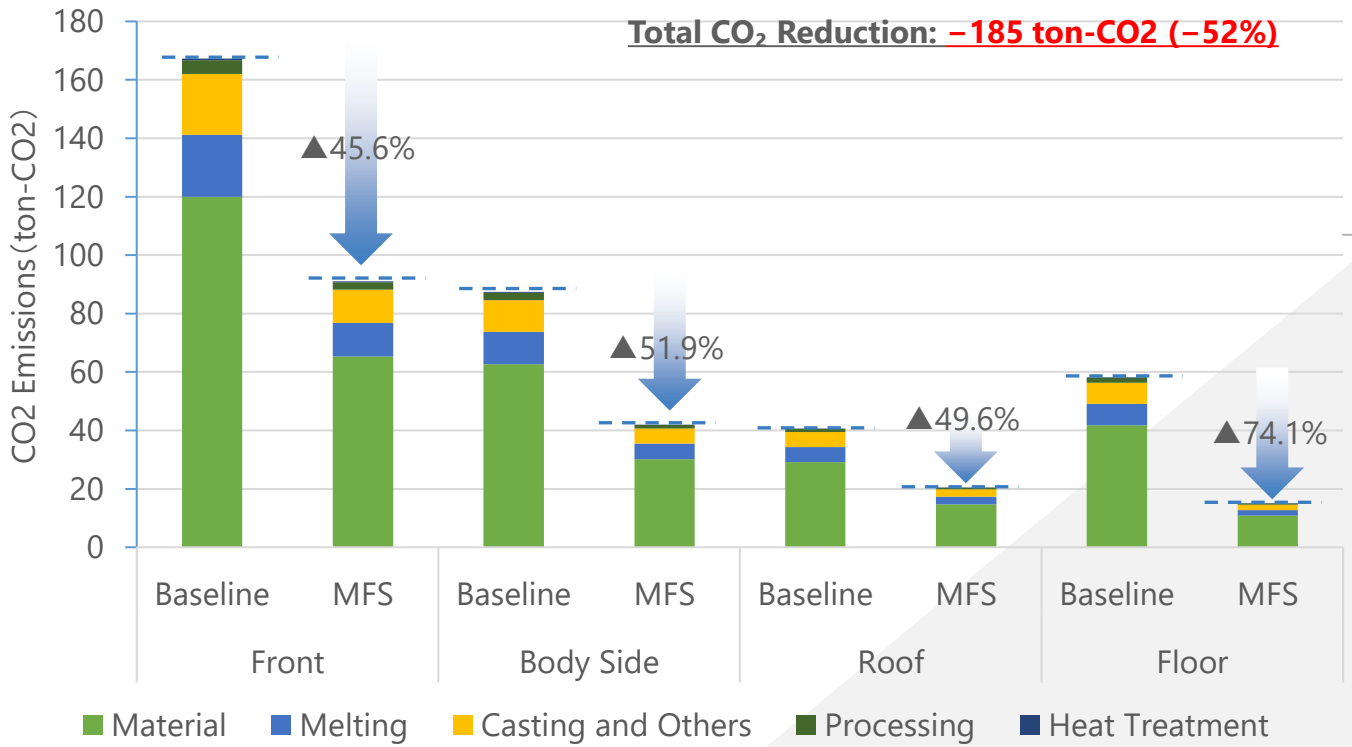

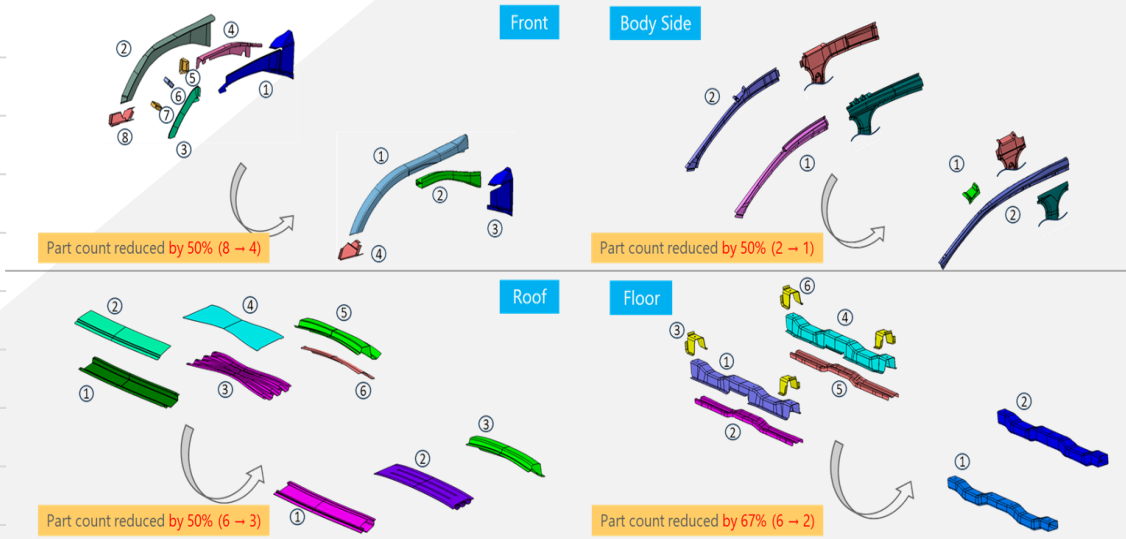

Notes

- Material EF is based on global average crude steel (Worldsteel).
- Casting yield is assumed to be 70% (literature-based typical value).
- Melting input is estimated as 1.035 × casting weight (induction furnace LCA).
- Machining allowance is approximated using a typical range (5–30%).
- Machining energy consumption is estimated based on a reference block machining dataset.
- Casting and other processes are allocated based on energy share (50.5% / 49.5%).
- Heat treatment is simplified and Furnace efficiency (η) is assumed to be 0.7, representing a typical industrial furnace performance.
- The die weight is estimated using a bounding-box approach with a filling ratio.
- Detailed geometry (e.g., pocketing, ribs, and local thickness variations) is not explicitly considered.
- The filling ratio (0.65) is an engineering assumption representing a non-solid die structure with pocketing and rib features.

Conclusions

GDIS

Future Works

- MFS concept demonstrated significant potential for vehicle lightweighting, performance enhancement, and CO_2 emissions reduction.
- Future work will extend MFS application to additional body structures not covered in this study, including B-pillar, C-pillar, and side sill, to further validate system-level benefits.
- Shape and surrounding component optimization will be pursued using decomposition-based structural synthesis methodologies to maximize MFS performance and integration efficiency.

For more information

Global Business Development Team Lead
Sumitomo Heavy Industries, Ltd.
Address
5100 Parkcenter Ave Dublin, OH 43017
Email: ryuichi.Funada@shi-g.com
Phone: (614) 896-0282

Professor, Mechanical Engineering
University of Michigan
Address
2454 GGB, 2350 Hayward, Ann Arbor, MI 48109
Email: kazu@umich.edu
Phone: (734) 763-0036

<Acknowledgements>
We gratefully acknowledge the contributions of the following University of Michigan student researchers to modeling, analysis, and preparation of this work:

- Chenghao Li
- Khushal Khatri
- Shrujal Rajesh Zala
- Bhumi Kirankumar Patel